Coherence versus incoherence: Collapse and revival in a simple quantum model

N. B. Narozhny,* J. J. Sanchez-Mondragon,† and J. H. Eberly
Department of Physics and Astronomy, University of Rochester, Rochester, New York 14627
(Received 18 January 1980)

We describe the temporal behavior of the dynamic elements of an exactly soluble quantum model. The model consists of a single two-level atom or spin interacting with a single mode of the quantized radiation field in the dipole approximation, the mode being initially in an arbitrary coherent state of excitation. We give new long-time numerical and closed-form approximate analytic solutions for the expectation values of the atomic dipole moment and the difference in population of the two atomic levels in the rotating wave approximation. The atomic dipole-dipole correlation function is calculated. All of the results are obtained without semiclassical or decorrelation approximations. Unusual features found in the temporal behavior of this lossless model problem are "collapse," i.e., episodic nonexponential damping of both the atomic inversion and dipole moment, and two kinds of "revival" or partial recorrelation, in the dynamic evolution, during which the initial state is nearly recovered. We give analytic formulas for the collapse function, for both of the revival times, and for the envelope of the revival maxima. Some remarks are made about the nature of irreversibility in this exactly soluble and loss-free model.

I. INTRODUCTION

The simplest fully quantum-mechanical model problem involving the interaction of radiation and matter is almost certainly the interaction of one mode of a quantized radiation field with a single charged harmonic oscillator. In the dipole approximation the coupled Heisenberg equations of motion for the two degrees of freedom are, however, completely linear in this case and the problem is only a trivial exercise.

An extremely simple but still unsolved model problem is posed if the harmonic oscillator is replaced by a two-level atom. In 1958 Jaynes[1] used the rotating wave approximation[2] (RWA) to reduce it to an exactly solvable model. Jaynes and Cummings[3] subsequently discussed the properties of the solutions in relation to the corresponding solutions obtained if the radiation mode is not quantized. It is the exactly soluble RWA model that we call the Jaynes-Cummings model.

We consider various features of the Jaynes-Cummings model[3] that arise when the field mode is prepared initially in a coherent state. For definiteness we will refer to this as the "coherent-state Jaynes-Cummings model". In this case the temporal behavior of the principal dynamic variables (atomic level populations, dipole moment, etc.) consists of Rabi oscillations. The envelopes of these oscillations collapse to zero despite the exactly loss-free nature of the model. We consider the long- and short-time behavior of the atomic dynamics and give an expression for the collapse function. We find that there are regular revivals, or quasirecorrelations, in the time records of the dynamical variables, and we give simple finite analytic expressions for both the revival period and the amplitude of the revival envelope.[4]

In the remainder of this section we will review the basic properties of the Jaynes-Cummings model, and mention previous work with it and with extensions of it. The remaining sections are devoted to, first, a review of Ackerhalt's operator solutions for relevant dynamical variables and a derivation of the atom's dipole-dipole correlation function (Sec. II), then a treatment of the long-time collapse and revival behavior of the inversion and the atomic dipole moment (Secs. III and IV), and finally a summary and discussion of results (Sec. V).

The Hamiltonian of the exactly soluble Jaynes-Cummings model is

$$H = \tfrac{1}{2}\hbar\omega_0\sigma_3 + \hbar\lambda(\sigma_+ a + a^\dagger\sigma_-) + \hbar\omega(a^\dagger a + \tfrac{1}{2}) . \quad (1.1)$$

Here the σ's are the usual 2×2 Pauli matrices satisfying

$$[\sigma_3, \sigma_\pm] = \pm 2\sigma_\pm , \quad [\sigma_+, \sigma_-] = \sigma_3 , \quad (1.2)$$

and a and $a^\dagger$ are the Bose operators for the quantized field mode which obey

$$[a, a^\dagger] = 1 . \quad (1.3)$$

The natural transition frequency ω_0 of the atom need not coincide with the mode frequency ω, although the rotating wave approximation is reliable only if $|\omega_0 - \omega| \ll \omega_0, \omega$. We denote the field-atom frequency difference by Δ:

$$\Delta = \omega_0 - \omega \quad (1.4)$$

and we refer to Δ as the detuning parameter.

The energy-level structure implied by the Jaynes-Cummings model is shown in Fig. 1 for $\lambda = 0$, that is, for uncoupled atom and field. When the coupling is turned on, it connects only the

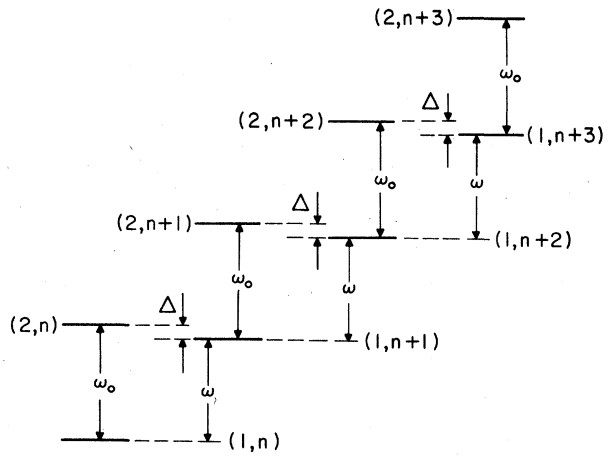

FIG. 1. Energy-level structure of the Jaynes-Cummings model. The atomic states are labeled by the atomic eigenvalue $m=-1$ (ground state 1) and $m=+1$ (excited state 2). Quantum-mechanical field variables are characterized by the photon-number eigenvalue n.

pairs of nearly degenerate levels separated by Δ. The exact eigenfrequencies for the two levels shown are

$$\omega_{nm}^{(\pm)} = N_{nm}\omega + \tfrac{1}{2}[\Delta \pm (\Delta^2 + 4\lambda^2 N_{nm})^{1/2}], \tag{1.5}$$

where N_{nm} is the "excitation number" for the coupled system

$$N_{nm} = n + \tfrac{1}{2}(m+1) \tag{1.6}$$

and only the lower sign in (1.5) is to be used when $N_{nm}=0$. Here $n=0,1,2,\ldots$, and $m=\pm 1$ are the eigenvalues of the unperturbed operators $a^\dagger a$ and σ_3, as usual. The exact eigenstates are linear combinations of the free eigenstates $|n,m\rangle$ and have been given by Jaynes.[1] These exact "dressed" states can be of great importance in any problem that has the Jaynes-Cummings[3] model at its core. We may mention strong-field resonance fluorescence as a recent example.

A number of extensions of the Jaynes-Cummings model have been carefully studied. The coupling of N two-level atoms to a single quantized radiation mode has been solved. Finite algorithms for the eigenfrequencies and eigenstates were given for $\Delta=0$ by Tavis and Cummings.[5] References to subsequent work may be found in the papers of Weiss[6] and of Compagno and Persico.[6] The coupling of a single two-level atom to M equal-frequency modes has been used as a simple model of decay processes, and solved by Quattropani.[7] It is apparently still an unsolved problem to find the eigenstates and eigenfrequencies of the N-atom + M-mode interaction.

In previous studies of long-time atomic dynamics and of field statistics in the one-atom one-mode Jaynes-Cummings model, interesting features due to coherent-state excitation of the cavity were noticed. A paper by Cummings[8] first touched this subject in 1965. Numerical evaluations of $\langle a^\dagger(t)a(t)\rangle$ and $\langle a^\dagger(t)\rangle\langle a(t)\rangle$ were compared. Cummings also obtained explicitly the Gaussian decay envelope associated with strong coherent excitation:

$$\exp[-\tfrac{1}{2}(\lambda t)^2], \tag{1.7}$$

and he commented on the different dynamical behavior arising from coherent and thermal excitation. We give an interpretation and generalization of (1.7) in Sec. III.

In a well-known review,[9] Stenholm gave explicit expressions for the time dependence of all elements of the density matrix of the coherent-state Jaynes-Cummings atom. All of these expressions contain infinite sums. Stenholm displayed graphs of the results of numerical evaluations of these sums, showing that decay exists in the model, even though it is lossless. However, both the graphs and their interpretation require correction. Later, in 1975, von Foerster[10] gave equivalent expressions and accurate graphs of the occupation probabilities for the atomic ground state for long and short times, but without interpretation. von Foerster also obtained infinite series expressing aspects of the cavity-mode statistics.

Meystre, Quattropani *et al.*, in a series of overlapping papers,[11-13] also studied the atomic dynamics and field statistics when the field mode is initially in a coherent state. They observed in numerical calculations[11] that decay occurs in this loss-free model and is independent of the average number of photons in the cavity, and they rederived Cummings's Gaussian decay envelope (1.7). However, on the basis of numerical work, they proposed that some variables (the expectation of the atomic dipole moment, in particular) appear to be immune to permanent decay. We will show below that this proposal must be rejected in light of the quasirecurrences that we find. One conclusion of the work mentioned in Ref. 13 was that the behavior of real physical systems can be described by the coherent-state Jaynes-Cummings model solutions only for times small compared with their damping times. This conclusion also seems to require modification.

II. OPERATOR SOLUTIONS AND DIPOLE-DIPOLE CORRELATION FUNCTION

In 1974 Ackerhalt[14] took a step in a new direction, with respect to the Jaynes-Cummings model, and presented the complete operator solutions for the evolution of the basic atomic and field-mode variables. These Heisenberg-picture solu-

tions are particularly valuable for a study of the coherence properties of the model because they make it a straightforward matter to construct unequal-time correlation functions.

Following Ackerhalt, we use two constants of motion repeatedly. These are the "excitation number" $\hat{N}$:

$$\hat{N}=\hat{a}^{\dagger}\hat{a}+\hat{\sigma}_{+}\hat{\sigma}_{-}, \tag{2.1}$$

and the "exchange constant" $\hat{C}$:

$$\hat{C}=\tfrac{1}{2}\Delta\hat{\sigma}_{3}+\lambda(\hat{a}^{\dagger}\hat{\sigma}_{-}+\hat{\sigma}_{+}\hat{a}). \tag{2.2}$$

As Ackerhalt shows,[14] the Heisenberg equations for $\hat{a}(t)$ and $\hat{\sigma}_{-}(t)$ are the same:

$$\left(i\frac{d}{dt}-\omega\right)\left(i\frac{d}{dt}-\omega+2\hat{C}\right)\begin{Bmatrix}\hat{\sigma}_{-}\\ \hat{a}\end{Bmatrix}=\lambda^{2}\begin{Bmatrix}\hat{\sigma}_{-}\\ \hat{a}\end{Bmatrix}, \tag{2.3}$$

and the solutions can be written

$$\begin{aligned}\hat{a}(t)e^{i\omega t}&=e^{i\hat{C}t}\left[\left(-\cos\hat{\gamma}t+i\hat{C}\frac{\sin\hat{\gamma}t}{\hat{\gamma}}\right)\hat{a}(0)+i\lambda\frac{\sin\hat{\gamma}t}{\hat{\gamma}}\hat{\sigma}_{-}(0)\right],\\ \hat{\sigma}_{-}(t)e^{i\omega t}&=e^{i\hat{C}t}\left[\left(\cos\hat{\gamma}t+i\hat{C}\frac{\sin\hat{\gamma}t}{\hat{\gamma}}\right)\hat{\sigma}_{-}(0)-i\lambda\frac{\sin\hat{\gamma}t}{\hat{\gamma}}\hat{a}(0)\right],\end{aligned} \tag{2.4}$$

where $\hat{\gamma}$ is a constant operator

$$\hat{\gamma}=[\tfrac{1}{4}\Delta^{2}+\lambda^{2}(\hat{N}+1)]^{1/2}, \tag{2.5}$$

which commutes with the operator $\hat{C}$

$$[\hat{C},\hat{\gamma}]=0. \tag{2.6}$$

We will now use the solutions (2.4) to construct the dipole-dipole correlation function

$$\langle\alpha,m|\hat{\sigma}_{+}(t)\hat{\sigma}_{-}(t')|\alpha,m\rangle, \quad m=\pm 1 \tag{2.7}$$

where the states $|\alpha,m\rangle$ are the direct product of free ($\lambda=0$) atomic states $|m\rangle$ and coherent states of the radiation field $|\alpha\rangle$ with complex amplitudes α:

$$\hat{a}(0)|\alpha\rangle=\alpha|\alpha\rangle. \tag{2.8}$$

The atomic eigenvalue $m=-1$ corresponds to the ground state and $m=+1$ to the excited state of the atom:

$$\begin{aligned}&\hat{\sigma}_{-}(0)|-1\rangle=0, \quad \hat{\sigma}_{-}(0)|1\rangle=|-1\rangle,\\ &\hat{\sigma}_{+}(0)|-1\rangle=|1\rangle, \quad \hat{\sigma}_{+}(0)|1\rangle=0.\end{aligned} \tag{2.9}$$

The operators $\hat{\gamma}$ and $\hat{C}^{2}$ are diagonal with respect to the atomic states while $\hat{C}$ is not:

$$\hat{C}|\alpha,-1\rangle=-\tfrac{1}{2}\Delta|\alpha,-1\rangle+\lambda\alpha|\alpha,1\rangle. \tag{2.10}$$

Taking into account relations (2.8)–(2.10) and commutation relation (2.6), we can rewrite both correlation functions (2.7) in the following way:

$$\begin{aligned}&\langle\alpha,m|\hat{\sigma}_{+}(t)\hat{\sigma}_{-}(t')|\alpha,m\rangle\\ &=e^{i\omega s}\left\langle\alpha,-1\left|\left(\cos\hat{C}s+\tfrac{1}{2}i\Delta\frac{\sin\hat{C}s}{\hat{C}}\right)\right.\right.\\ &\quad\left.\left.\times\Lambda_{m}^{*}(t)\Lambda_{m}(t')\frac{\sin\hat{\gamma}t}{\hat{\gamma}}\frac{\sin\hat{\gamma}t}{\hat{\gamma}}\right|\alpha,-1\right\rangle,\end{aligned} \tag{2.11}$$

where $s=t-t'$ and

$$\Lambda_{m}(t)=\begin{cases}\lambda\alpha, & m=-1\\ i\dfrac{d}{dt}+\dfrac{1}{2}\Delta, & m=1.\end{cases} \tag{2.12}$$

If we now represent the states $|\alpha,m\rangle$ as a superposition of states with definite numbers of photons

$$|\alpha,m\rangle=\sum_{n=0}^{\infty}|n,m\rangle\langle n|\alpha\rangle \tag{2.13}$$

with

$$\langle n|\alpha\rangle=\exp(-\tfrac{1}{2}|\alpha|^{2})\alpha^{n}/\sqrt{n!}, \tag{2.14}$$

and take into account the diagonality of the operator on the right side of equation (2.11) with respect to both atomic and photon states, we easily get

$$\langle\alpha,m|\sigma_{+}(t)\sigma_{-}(t')|\alpha,m\rangle=\exp(-|\alpha|^{2}+i\omega s)\sum_{n=0}^{\infty}\frac{|\alpha|^{2n}}{n!}[\cos\nu_{n}'s+i(\Delta/2\nu_{n}')\sin\nu_{n}'s]\Lambda_{m}^{*}(t)\Lambda_{m}(t')\nu_{n}^{-2}\sin(\nu_{n}t)\sin(\nu_{n}t'), \tag{2.15}$$

where

$$\begin{aligned}\nu_{n}'&=(\tfrac{1}{4}\Delta^{2}+\lambda^{2}n)^{1/2},\\ \nu_{n}&=[\tfrac{1}{4}\Delta^{2}+\lambda^{2}(n+1)]^{1/2}.\end{aligned} \tag{2.16}$$

Finally after trivial transformations we can write

$$\begin{aligned}\langle\alpha,m|\sigma_{+}(t)\sigma_{-}(t-s)|\alpha,m\rangle&=\exp(-|\alpha|^{2}+i\omega s)\sum_{n=0}^{\infty}\frac{|\alpha|^{2n}}{n!}[\Delta^{2}+4\lambda^{2}(n+1)]^{-1/2}[\cos\nu_{n}'s+i(\Delta/2\nu_{n}')\sin\nu_{n}'s]\\ &\quad\times[A_{m}(\nu_{n})e^{i\nu_{n}s}+A_{m}(-\nu_{n})e^{-i\nu_{n}s}-2B_{m}(n)\cos\nu_{n}(s-2t)],\end{aligned} \tag{2.17}$$

where

$$A_m(\nu_n)=\begin{cases}\lambda^2|\alpha|^2, & m=-1\\ (\nu_n+\frac{1}{2}\Delta)^2, & m=1\end{cases} \tag{2.18}$$

$$B_m(n)=\begin{cases}\lambda^2|\alpha|^2, & m=-1\\ -\lambda^2(n+1), & m=1.\end{cases} \tag{2.19}$$

The dependence of the correlation function on t as well as on s leads to interesting effects. In the first place, the inversion $\langle\sigma_3(t)\rangle$ is not constant in time. Its time dependence is examined in the next section. In the second place, the Wiener-Khintchine relation cannot be used to calculate the spectrum from the correlation function. The consequences of this will be discussed in a subsequent paper.

III. ATOMIC INVERSION

The degree of atomic inversion is perhaps the simplest nontrivial physical quantity in the Jaynes-Cummings problem. Its dynamical behavior in a photon-number state was found by Jaynes[1] to be purely sinusoidal. For short times its behavior in a coherent initial state is also known analytically.[12] We now extend these latter results. The inversion may be written

$$\begin{aligned}W_m(t)&=\langle\alpha,m|\hat{\sigma}_3(t)|\alpha,m\rangle\\&=1-2\langle\alpha,m|\hat{\sigma}_+(t)\hat{\sigma}_-(t)|\alpha,m\rangle\end{aligned} \tag{3.1}$$

and with the help of formula (2.17) one can easily get the result $W_m(t)=\langle m|\hat{\sigma}_3(0)|m\rangle w_m(t)$, where $w_m(t)$ is obviously the ratio of inversion to initial inversion:

$$w_m(t)=e^{-|\alpha|^2}\sum_{n=0}^{\infty}\frac{|\alpha|^{2n}}{n!}\times\left(1-8\frac{\lambda^2[n+\frac{1}{2}(m+1)]}{\Omega_{nm}^2}\sin^2(\tfrac{1}{2}\Omega_{nm}t)\right). \tag{3.2}$$

This is seen to be simply a sum, with Poisson weights, of the known off-resonant results for different n states; and the oscillation frequency

$$\Omega_{nm}^2=\Delta^2+4\lambda^2[n+\tfrac{1}{2}(m+1)] \tag{3.3}$$

may be called the quantum-electrodynamic (QED) Rabi frequency.[15] The sum appears to have no known analytic expression, for any values of the parameters α, Δ, and m, so long as $\lambda\neq 0$.

In the case $|\alpha|^2\equiv\bar{n}\gg 1$ the summation over n in (3.2) can be performed approximately, using saddle-point techniques, with the help of the Euler-Maclaurin formula[16] if one notices that the weighting factor $P(n)=e^{-\bar{n}}\bar{n}^n/n!$ will peak at a value $n=\bar{n}$ with relatively narrow dispersion: $(\langle n^2\rangle-\bar{n}^2)^{1/2}=\sqrt{\bar{n}}$. This means that the sum in (3.2) can be changed to an integral which after trivial transformations can be written as

$$w(t)\simeq\int_0^{\infty}\frac{dn}{\Omega^2(n)}P(n)[\Delta^2+4\lambda^2 n\cos\Omega(n)t], \tag{3.4}$$

with

$$P(n)=(2\pi n)^{-1/2}\exp[-\bar{n}+n-n\ln(n/\bar{n})] \tag{3.5}$$

and

$$\Omega^2(n)=\Delta^2+4\lambda^2 n. \tag{3.6}$$

Note that in the limit $\bar{n}\gg 1$ the inversion W depends on the initial atomic state only through $\langle m|\sigma_3(0)|m\rangle$ and the index m may be omitted from w.

Using the saddle-point method for evaluating the integral (3.4) one can get

$$w(t)\simeq\frac{\Delta^2}{\Omega^2(\bar{n})}\left(1+\frac{4\lambda^2\bar{n}}{\Delta^2}\,\mathrm{Re}\frac{\exp[-\bar{n}+\bar{n}\psi(\eta_0)]}{\sqrt{\psi''(\eta_0)}}\right), \tag{3.7}$$

where

$$\begin{aligned}\psi(\eta)&=\eta(1-\ln\eta)\\&\quad+i2\lambda\bar{n}^{-1/2}t(\eta+\Delta^2/4\lambda^2\bar{n})^{1/2},\end{aligned} \tag{3.8}$$

with $\eta=n/\bar{n}$. Here η_0 is a solution of the equation

$$\psi'(\eta_0)=0,$$

or

$$(\eta_0+\Delta^2/4\lambda^2\bar{n})^{1/2}\ln\eta_0=i\lambda\bar{n}^{-1/2}t, \tag{3.9}$$

and thus η_0 depends on time. Since $(\bar{n})^{1/2}$ as well as $\bar{n}$ are considered to be very large, the time-dependent term in (3.7) will be exponentially small if η_0 fails to satisfy the condition

$$|1-\mathrm{Re}\psi(\eta_0)|\ll\bar{n}^{-1/2}. \tag{3.10}$$

Now we can see that for very short times $t\ll t_0$, where

$$t_0=\lambda^{-1}(1+\Delta^2/4\lambda^2\bar{n})^{1/2}, \tag{3.11}$$

Eq. (3.9) has a trivial solution $\eta_0=1$ and $\mathrm{Re}\psi(1)=1$. The dominant dynamical behavior of (3.7) is then governed by $i\bar{n}\,\mathrm{Im}\psi(1)$, and this behavior is simple sinusoidal oscillation at the Rabi frequency (3.6). But when $t\sim t_0$, η_0 as well as $\mathrm{Re}\psi(\eta_0)$ differ from 1 by terms of order $(\bar{n})^{-1/2}$ and the second term in the large parentheses in (3.7) becomes exponentially small. The envelope of the sinusoidal oscillations then "collapses" rapidly to zero. Therefore t_0 can be considered to be the natural "collapse time" for Rabi-type oscillations in a two-level atom interacting with a single-mode radiation

field initially in a pure coherent state.

This collapse has a simple physical meaning. The inversion is the sum (3.2) of terms which represent Rabi oscillations of the inversion due to emission and absorption of definite numbers of photons n. At the moment $t=0$ the system is prepared in a definite state and therefore all these processes are then correlated. But since all terms in (3.2) oscillate with different frequencies (3.4) they will become decorrelated in a time t_0 associated with the range of frequencies that make significant contributions to the sum. This decorrelation time t_0 is easily seen to be estimated by

$$[\Omega(\bar{n}+\bar{n}^{1/2})-\Omega(\bar{n}-\bar{n}^{1/2})]t_0 \sim 1, \tag{3.12}$$

if $\bar{n} \gg 1$. Considering $\bar{n}^{1/2} \ll \bar{n}$ we get

$$t_0 \sim \lambda^{-1}(1+\Delta^2/4\lambda^2\bar{n})^{1/2}$$

in agreement with (3.11). Under conditions of exact resonance $\Delta=0$, this collapse time has been found by Cummings[8] and Meystre *et al.*[12] We may point out also that our approach replaces Cummings's expression (1.7) with a more general "collapse function", and at the same time suggests that the factor $\frac{1}{2}$ in Cummings's exponent has a physical interpretation. The collapse function replacement mandated by (3.11) is

$$\exp[-\tfrac{1}{2}(\lambda t)^2] \to \exp[-p_2(\lambda t)^2], \tag{3.13}$$

where

$$p_2 = 2\lambda^2\bar{n}/(\Delta^2+4\lambda^2\bar{n}). \tag{3.14}$$

One recognizes p_2 as the steady-state probability that the atom is in its upper state. [Compare with the steady-state value (first term) of $w=2p_2-1$ in (3.7) or the time average of w in Eq. (3.18) of Ref. 15.]

In addition to the collapse of its Rabi oscillations, the time behavior of the inversion has another even more interesting feature. As time increases we actually encounter a revival of the collapsed $w(t)$, in fact an infinite sequence of collapses and revivals. They take place when the phases of oscillation of neighboring terms in (3.2) differ by the factor 2π for $n \sim \bar{n}$. That is, the interval T_R between revivals can be found from the relation

$$[\Omega(\bar{n}+1)-\Omega(\bar{n})]T_R \cong 2\pi, \tag{3.15}$$

or

$$T_R \equiv 2\pi\lambda^{-1}\bar{n}^{1/2}(1+\Delta^2/4\lambda^2\bar{n})^{1/2}. \tag{3.16}$$

One can easily check that this qualitative result is in agreement with Eq. (3.9), since at moments of time $t=kT_R$, Eq. (3.9) has exact solutions $\eta_0 = e^{i2\pi k}$, $k=0,1,2,\ldots$.

The time behavior of η_0 can be illustrated if we introduce a complex plane for η with a cut along the negative real axis. At $t=0$, $\eta_0=1$. Then it travels along the plane, goes to the second sheet and crosses the real axis on the second sheet at the moment of time $t=T$ and so on. Though the function $\eta_0(t)$ is not periodic, the zeroes of the function $[\eta_0(t)-1]$ are periodic in t with the period T given by formula (3.16).

The above analysis shows that it would be enough to find the "local" solutions of Eq. (3.9) near the revival points $\eta_0(kT_R)=e^{i2\pi k}$, $k=0,1,2,\ldots$. One can look for these solutions in the form

$$\eta_{0k}(t) = \rho_k e^{i\varphi_k}, \quad \rho_k = 1+\rho_k^{(1)}, \quad \varphi_k = 2\pi k + \varphi_k^{(1)},$$

under the condition that the "local time" τ is small. That is, we assume

$$t = kT_R + \tau; \quad \rho_k^{(1)} \ll 1; \quad \varphi_k^{(1)} \ll 1;$$
$$\lambda\bar{n}^{-1/2}\tau(1+\Delta^2/4\lambda^2\bar{n})^{-1/2} \ll 1.$$

These solutions are

$$\varphi_k^{(1)} = \lambda\bar{n}^{-1/2}\tau\left(1+\frac{\Delta^2}{4\lambda^2\bar{n}}\right)^{-1/2}\left[1+\left(\frac{\pi k}{1+\Delta^2/4\lambda^2\bar{n}}\right)^2\right]^{-1}, \tag{3.17}$$

$$\rho_k^{(1)} = \lambda\bar{n}^{-1/2}\tau\pi k\left(1+\frac{\Delta^2}{4\lambda^2\bar{n}}\right)^{-3/2} \times\left[1+\left(\frac{\pi k}{1+\Delta^2/4\lambda^2\bar{n}}\right)^2\right]^{-1}. \tag{3.18}$$

With the help of these last formulas we can now write formula (3.7) for the inversion in the form

$$w(t) \simeq \frac{\Delta^2}{\Omega^2(\bar{n})} + \frac{4\lambda^2\bar{n}}{\Omega^2(\bar{n})}\left(1+16\frac{\lambda^8\bar{n}^2t^2}{\Omega^6(\bar{n})}\right)^{-1/4} \times\exp[-\Psi(t)]\cos\Phi(t), \tag{3.19}$$

$$\Psi(t) = 2\bar{n}\sin^2\left(\frac{\lambda^2 t}{\Omega(\bar{n})}\right)\left(1+16\frac{\lambda^8\bar{n}^2t^2}{\Omega^6(\bar{n})}\right)^{-1}, \tag{3.20}$$

$$\Phi(t) = \Omega(\bar{n})t + \bar{n}\sin[2\lambda^2 t/\Omega(\bar{n})] - 2\lambda^2\bar{n}t/\Omega(\bar{n}) - \tfrac{1}{2}\arctan[4\lambda^4\bar{n}t/\Omega^3(\bar{n})], \tag{3.21}$$

where $\Omega(\bar{n})$ is represented by formula (3.6). To obtain formula (3.20) we have substituted $\sin[\lambda^2 t/\Omega(\bar{n})]$ for $\lambda^2\tau/\Omega(\bar{n})$. Such a substitution is useful in our approximation to indicate the periodicity of the revivals. This substitution is not unique, of course, and the figures included below show that (3.20) does not represent the wings of the revival regions with great accuracy, but the

positions and central portions of these regions are modeled well.

The nature of the revivals, and many of the features of $w(t)$ and the approximate formula (3.19), are apparent in Figs. 2–4. The short-time behavior of $w(t)$ for very small $\bar{n}$ is presented in Fig. 2. The upper pictures correspond to a numerical computation of formula (3.2), and the analytical expression (3.19) for $w(t)$ is plotted in the lower pictures. The collapse function (3.13) is shown explicitly in both upper and lower pictures. One can see from the figure that the approximate formula for $w(t)$ begins to work when $\bar{n} \gtrsim 4$, and even for $\bar{n}$ so small the Rabi oscillations and the Gaussian collapse formula are well confirmed by the numerical evaluation.

Figure 3 presents the behavior of $w(t)$ for stronger initial coherent states. In Figure 3(b), for $\bar{n} = 900$, one can see the long-time behavior of $w(t)$ with many revivals inside the long-time bounding envelope $B(t)$:

$$B(t) = [1 + 16\lambda^8 \bar{n}^2 t^2/\Omega^6(\bar{n})]^{-1/4} . \tag{3.22}$$

The period of the revivals coincides with (3.13). Figure 3(a) shows the short-time behavior of $w(t)$, with many Rabi oscillations within the collapse envelope, for the same set of parameters. From comparison of this picture with the ones in Fig. 2 one can see that for small $\bar{n}$ the collapse envelope does depend on $\bar{n}$, even for $\Delta = 0$, in contrast to (3.13), which is valid for $\bar{n} \gg 1$. Figures 3(c) and 3(d), for $\bar{n} = 25$, show the structure of the first and second revivals, respectively. As one can see, by comparing upper and lower pictures in each of these figures, the approximate formula (3.19) correctly determines the position of the revivals and their structure near the center, but fails to represent correctly the width of the revivals.

Figure 4 is a three-dimensional picture of the short-time behavior of the inversion for $\bar{n} = 25$. The x axis is the time axis and the time range (in units of λ^{-1}) is 0 to π. The y axis is the detuning axis with the range 0 to 15. The initial state of the atom is the ground state. One can readily see the decrease in the amplitude of the Rabi oscillations as Δ increases. This is consistent with semiclassical results for the two-level problem.[15] A new feature shown in Fig. 4 is the lessening importance of the collapse function as Δ increases, as predicted in (3.13) and (3.14).

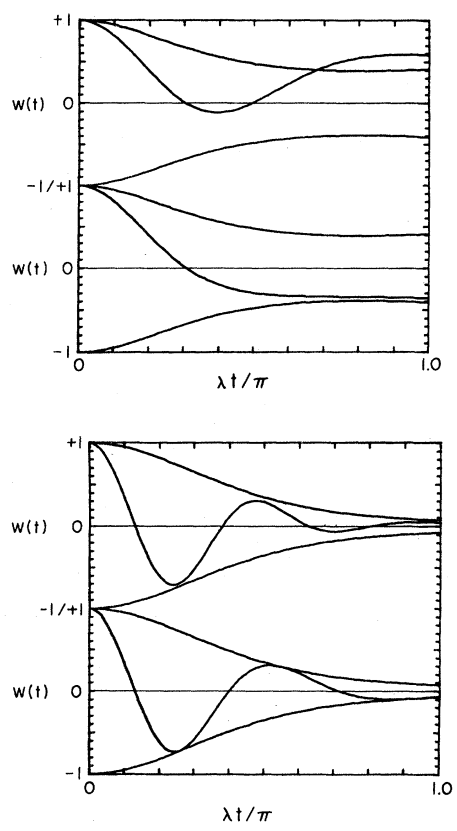

FIG. 2. Behavior of the atomic inversion $w(t)$ in the case of weak excitation. (a) Very small $\bar{n}$: $\bar{n} = 1$, $\lambda = 1$, and $\Delta = 0$. In this case the agreement between the analytical approximate solution (lower curve), and the numerical solution (upper curve) is poor. (b) Small $\bar{n}$: $\bar{n} = 4$, $\lambda = 1$, $\Delta = 0$. The agreement between the numerical solution (upper curve) and the approximate analytical solution (lower curve) is good. The envelopes in all the curves in (a) and (b) are given by formula (3.19). Time is measured in units of π/λ and $m = -1$.

IV. ATOMIC DIPOLE MOMENT

The dipole moment of the coherent-state Jaynes-Cummings atom may be treated in the same way as the inversion. We consider the quantity

$$D_m(t) = \langle \alpha, m | \sigma_-(t) e^{i\omega t} | \alpha, m \rangle , \tag{4.1}$$

which could be called the complex envelope of the dipole moment. The computation of $D_m(t)$ gives

$$D_m(t) = \frac{\lambda\alpha}{2} e^{-|\alpha|^2} \sum_{n=0}^{\infty} \frac{|\alpha|^{2n}}{n!} \left[\frac{2m\Delta}{\Omega_{nm}\Omega'_{nm}} [\cos\tfrac{1}{2}(\Omega'_{nm} - \Omega_{nm})t - \cos\tfrac{1}{2}(\Omega'_{nm} + \Omega_{nm})t] \right.$$
$$\left. + i\left(\frac{m+1}{\Omega_{nm}} + \frac{m-1}{\Omega'_{nm}}\right) \sin\tfrac{1}{2}(\Omega'_{nm} + \Omega_{nm})t - i\left(\frac{m+1}{\Omega_{nm}} - \frac{m-1}{\Omega'_{nm}}\right) \sin\tfrac{1}{2}(\Omega'_{nm} - \Omega_{nm})t \right] , \tag{4.2}$$

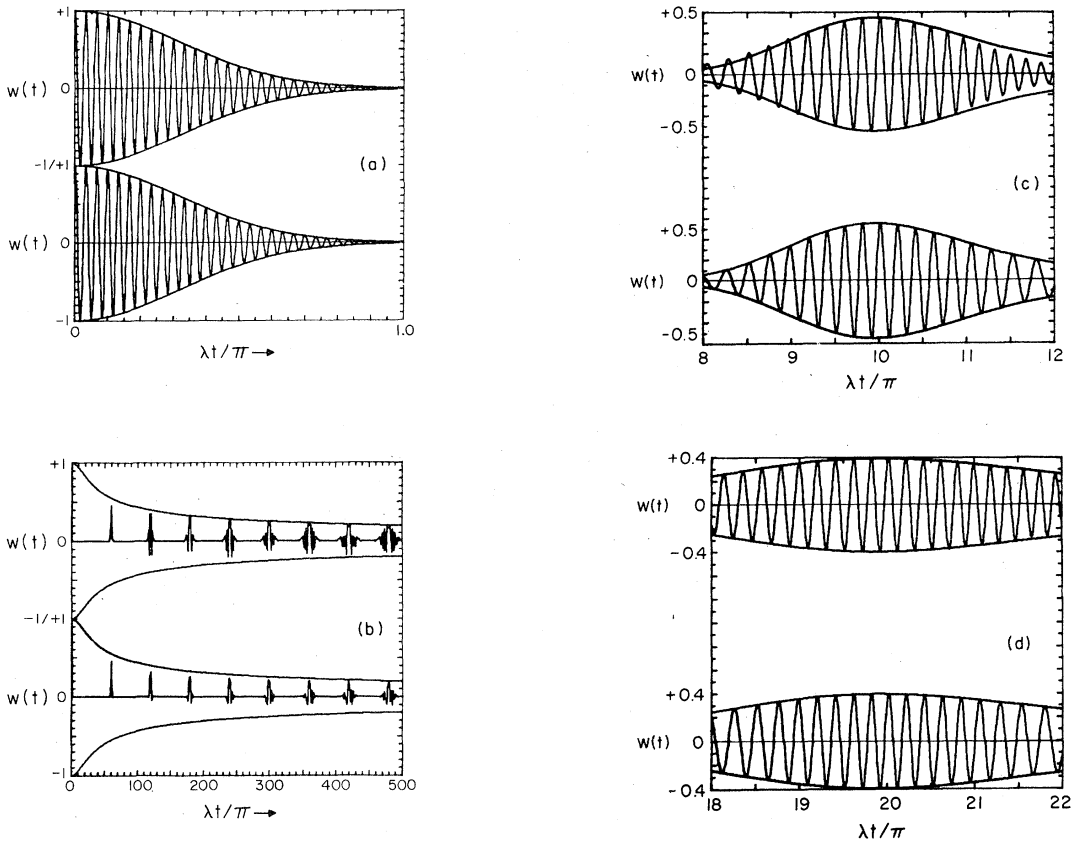

FIG. 3. Time evolution of the atomic inversion $w(t)$ in the case of strong excitation. (a) $\bar{n}=900$, $\lambda=1$, $\Delta=0$, short times: $\lambda t<\pi$. In this case the basic oscillation occurs at the Rabi frequency, and is subject to Gaussian collapse independent of $\bar{n}$. (b) Long times: The range of time is 500 times larger than in (a), and qualitatively new features appear. The long-time behavior is characterized by periodic revivals or quasirecorrelations with period $T=2\pi\bar{n}^{1/2}/\lambda$ and a non-Gaussian bounding envelope given by Eq. (3.22). The views in (c) and (d) are closeups of the first and second revivals for $\bar{n}=25$, $\lambda=1$, and $\Delta=0$. The basic oscillation in the revival zone occurs at the Rabi frequency, and is subject to an envelope of increasing width as a function of time and to overall long-time damping. Notice the excellent agreement between the numerical solution (upper curve) and the analytical approximate solution (lower curve) in (a). The agreement between the numeric and approximate analytic solutions shown in (b), (c), and (d) for the period of the Rabi oscillation and the period of the revivals is good, but our approximation is less accurate when determining the width of the revivals. Time is measured in units of π/λ and $m=-1$.

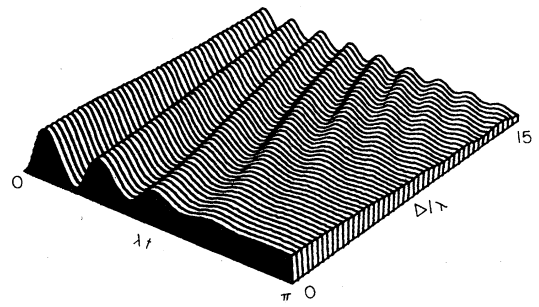

FIG. 4. Behavior of the atomic inversion $w(t)$ as a function of both time and the detuning. The slower collapse of off-resonance Rabi oscillations predicted by Eq. (3.12) is illustrated with $\bar{n}=25$, $\lambda=1$, and $m=-1$.

where the notation is the same as in the previous sections and

$$\Omega'^2_{nm}=\Omega^2_{n+1,m}=\Delta^2+4\lambda^2[n+1+\tfrac{1}{2}(m+1)]\,. \tag{4.3}$$

The function $D_m(t)$ can be divided into two parts

$$D_m(t)=D_m^{(f)}(t)+D_m^{(s)}(t)\,. \tag{4.4}$$

Here $D_m^{(f)}$ and $D_m^{(s)}$ denote, respectively, the fast and slow terms in (4.2) that have a sum or a difference of frequencies in the arguments of the trigonometric functions. For large $\bar{n}$ we find the following analytic expression in exactly the same way as for the function $w_m(t)$:

$$D_m^{(f)}(t) \simeq i\frac{\lambda\alpha m}{\Omega(\bar{n})}\left(1+16\frac{\lambda^8\bar{n}^2t^2}{\Omega^6(\bar{n})}\right)^{-1/4} \times e^{-\varphi(t)}\left(\sin\Phi(t)+i\frac{\Delta}{\Omega(\bar{n})}\cos\Phi(t)\right). \quad (4.5)$$

Expression (4.5) has of course some of the same features as the inversion; the same Gaussian collapse function, the same interval between revivals, and so on.

The behavior of the $D_m^{(s)}$ part of the complex dipole moment envelope differs from the behavior of the $D_m^{(f)}$ part because the frequency of its oscillating terms is significantly smaller. In this case we find

$$D_m^{(s)}(t) \simeq \lambda\alpha e^{-|\alpha|^2}\sum_{n=0}^{\infty}\frac{|\alpha|^{2n}}{n!}\left(\frac{m\Delta}{\Omega^2(n)}\cos\frac{\lambda^2}{\Omega(n)}t - i\frac{1}{\Omega(n)}\sin\frac{\lambda^2}{\Omega(n)}t\right), \quad (4.6)$$

where we used the assumption $\bar{n}\gg 1$ and therefore replaced $\Omega'_{nm}-\Omega_{nm}$ by $\lambda^2/\Omega(n)$.

Applying the same method of calculation we have used in the previous section to (4.6), we get

$$D_m^{(s)}(t) \simeq \lambda\alpha\exp\left[-\frac{\lambda^2t^2}{32\bar{n}^2}\left(1+\frac{\Delta^2}{4\lambda^2\bar{n}}\right)^{-3/2}\right] \times\left(\frac{m\Delta}{\Omega^2(\bar{n})}\cos\frac{\lambda^2}{\Omega(\bar{n})}t - i\frac{1}{\Omega(\bar{n})}\sin\frac{\lambda^2}{\Omega(\bar{n})}t\right). \quad (4.7)$$

The function $D_m^{(s)}(t)$ also has a Gaussian collapse function, but its decay time t_0' now depends on $\bar{n}$ and is much larger than the decay time of $D_m^{(f)}(t)$ (or of the inversion):

$$t_0' \sim \frac{4\bar{n}}{\lambda}\left(1+\frac{\Delta^2}{4\lambda^2\bar{n}}\right)^{3/4} \quad (4.8)$$

and its period of oscillation is given by

$$T = \frac{4\pi}{\lambda}\sqrt{\bar{n}}\left(1+\frac{\Delta^2}{4\lambda^2\bar{n}}\right) = 2T_R, \quad (4.9)$$

i.e., double the period of revival found for both the inversion and $D_m^{(f)}(t)$. The function $D_m^{(s)}(t)$ has its own time of revival T_R' which can be found from the condition

$$\frac{\lambda^2}{\Omega(\bar{n})}-\frac{\lambda^2}{\Omega(\bar{n}+1)}=\frac{2\pi}{T_R'}, \quad (4.10)$$

[compare with (3.16)] and is equal to

$$T_R' = \frac{8\pi}{\lambda}\bar{n}^{3/2}\left(1+\frac{\Delta^2}{4\lambda^2\bar{n}}\right)^{3/2}. \quad (4.11)$$

In order to illustrate the analytic features derived above we have chosen some representative cases to present graphically. The graphs were obtained by numerical summation. In Fig. 5 we show the case previously presented both by Stenholm[9] and by Meystre *et al.*,[11,13] i.e., $\alpha=3$ and at exact resonance. Both $D_m^{(f)}(t)$ and $D_m^{(s)}(t)$ are complex, and their real (dispersive) parts vanish at resonance. Figure 5 shows the imaginary (absorptive) parts of $D_m^{(f)}(t)$ and $D_m^{(s)}(t)$ separately and also the sum. The nonzero value of the sum for times longer than t_0 is due first to the slow collapse of the initial coherence in $D_m^{(s)}$, and then to the first revival of the rapidly oscillating $D_m^{(f)}$.

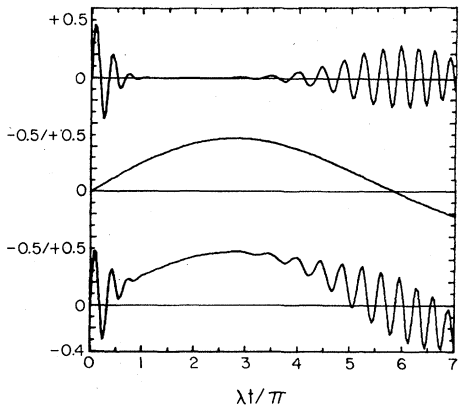

FIG. 5. Short-time behavior of the envelope $D_m(t)$ of the on-resonance complex dipole moment. In this case the real part is zero. The three curves, from top to bottom are $D_m^{(f)}(t)$ the inversionlike component, $D_m^{(s)}(t)$ the slowly varying component, and the total $D_m(t)$ $=D_m^{(f)}(t)+D_m^{(s)}(t)$. The time is given in units of π/λ and $\bar{n}=9$, $\lambda=1$, $\Delta=0$, $m=-1$.

For the case $\alpha=3$ and $\Delta=0$, formula (4.8) predicts that $D_m^{(s)}$ will decay by $e^{-2}\simeq 0.14$ after the relatively long time $t_0'\sim 72/\lambda\simeq 25\pi$. This is shown to be the case in Fig. 6. One also sees in Fig. 6

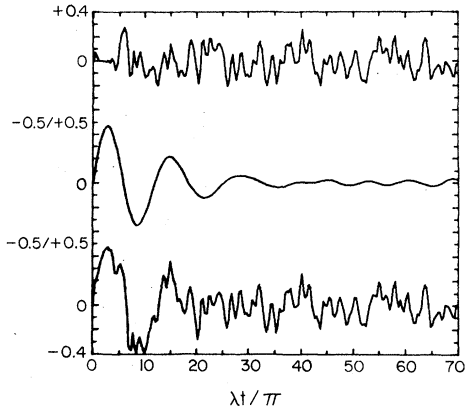

FIG. 6. Long-time dependence of the envelope of the on-resonance complex dipole moment. From top to bottom $D_m^{(f)}(t)$, $D_m^{(s)}(t)$, $D_m(t)$. Notice the $\bar{n}$-dependent Gaussian collapse of $D_m^{(s)}(t)$. Time is measured in units of π/λ and $\bar{n}=9$, $\lambda=1$, $\Delta=0$, $m=-1$.

the highly random apparently irreversible incoherent behavior of $D_m(t)$ for times longer than t_0'. However, our approximate analysis of the exact sum (4.2) predicts that $D_m^{(s)}$ will also experience quasirecorrelation of its oscillations. Such quasirecorrelation does occur, and the first revival in the case $\alpha = 10$, $\Delta = 0$, is shown in Fig. 7.

The effect of off-resonant excitation is also easily illustrated. We have chosen the same parameters as Stenholm, i.e., $\alpha = 3$ and $\Delta = 2\lambda$. In Fig. 8 the time dependence of both the dispersive and absorptive parts of the dipole moment are shown. We find them to be very similar in behavior for this value of detuning Δ, in contrast to the behavior shown in Stenholm's Fig. 3.5.

Finally, the value of the revival period of the slowly collapsing slow oscillations of $D_m^{(s)}$ is predicted in (4.11). This is more of a challenge to illustrate because a comparison of (4.11) and (4.8) shows that the separation between revivals T_R' is only $(\bar{n})^{1/2}$ times as great as the revival half-width. Thus, in order to distinguish successive revivals from each other we require an example with $(\bar{n})^{1/2} \gg 1$, for example, $\bar{n} = 25$. This implies times of the order of $t/\pi \sim T_R/\pi \sim 1000\lambda^{-1}$. These values of $\bar{n}$ and t are considerably larger than those used in any previous computation, by an order of magnitude or more, and offer an opportunity to test our numerical procedures. Thus we have chosen a value somewhat larger still, $\bar{n} = 400$, to make the test more significant. In this case more than 1000 terms of the sum given in (4.2) are computed. The first revival point is predicted to be at $t/\pi = 64\,000\lambda^{-1}$. Figure 9 shows

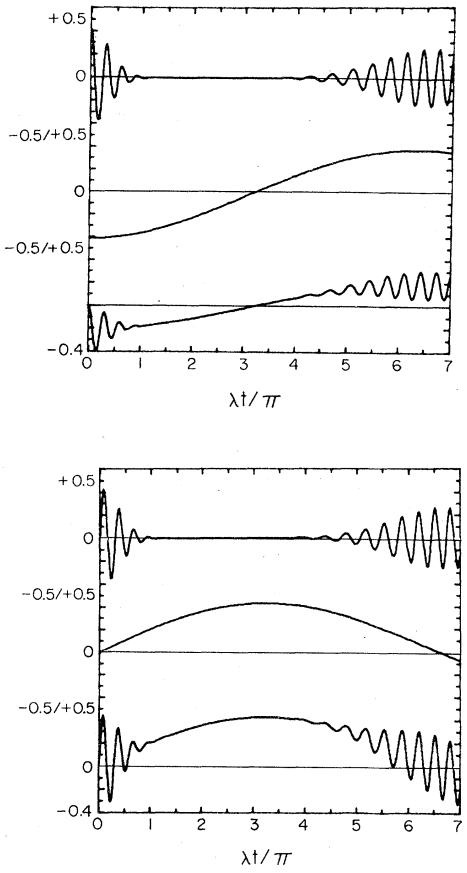

FIG. 8. Off-resonance complex dipole envelopes (a) real part of $D_m(t)$ and (b) imaginary part of $D_m(t)$. From top to bottom $D_m^{(f)}(t)$, $D_m^{(s)}(t)$, $D_m(t)$. Time is measured in units of π/λ and $\bar{n} = 9$, $\lambda = 1$, $\Delta = 2$, $m = -1$.

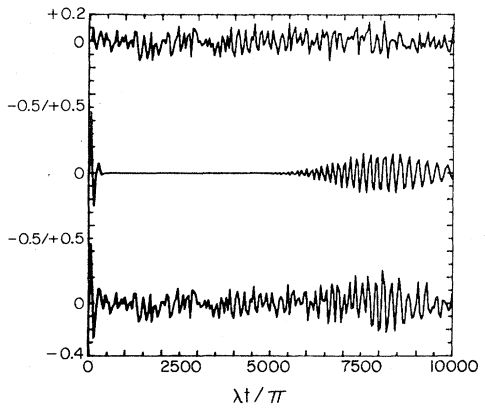

FIG. 7. Revivals of the on-resonance $D_m^{(s)}(t)$ for a strong initial field. From top to bottom: $D_m^{(f)}(t)$, $D_m^{(s)}(t)$, and $D_m(t)$. A new type of revival is shown for $D_m^{(s)}(t)$ with revival time $T_R' = (8\pi/\lambda)(\bar{n})^{3/2}$. Time is measured in units of π/λ and $\bar{n} = 100$, $\lambda = 1$, $\Delta = 0$, $m = -1$.

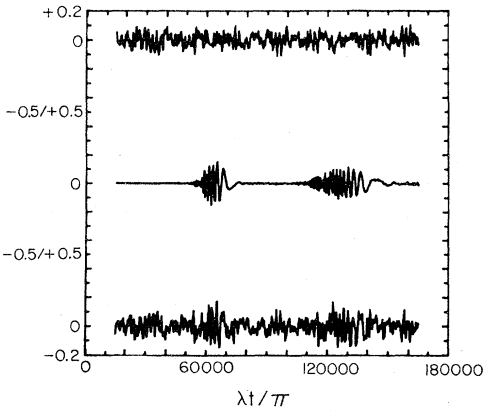

FIG. 9. Very long-time behavior of the dipole envelopes $D_m^{(f)}(t)$, $D_m^{(s)}(t)$, and $D_m(t)$. The revivals of $D_m^{(s)}(t)$ show variable width and long-time damping. Time is measured in units of π/λ and $\bar{n} = 400$, $\lambda = 1$, $\Delta = 0$, $m = -1$.

the first two revivals of the slow oscillations of $D_m^{(e)}$. They occur at the predicted points. Their amplitude is not great enough for the revivals to be readily visible in the sum $D_m^{(f)} + D_m^{(e)}$.

A last word concerning Figs. 7 and 9 is necessary. The extremely large range of times shown in each of these implies a fairly low graphic resolution, as only 301 plotting points were used to make the curves. Some amusing Moiré interferences can be arranged between the regular grid of plot points and the equally regular oscillations in $D_m(t)$ if desired. In the revival packets shown in Figs. 7 and 9, the apparent bunching of the packet oscillations to the right in Fig. 7 and to the left in Fig. 9 is an unintentional example of this. When examined much more closely, the internal structure of the revival packets of the dipole moment is equally as uniform as those shown for the inversion in Fig. 2(a).

V. SUMMARY AND DISCUSSION

Exactly soluble and fully quantum-mechanical models are rare. The Jaynes-Cummings model has been studied many times because of the relatively realistic way that it represents the actual dipole coupling of an atom to a quantized radiation field. From this model one hopes to learn, for example, about the coherence properties of the quantized *interacting* radiation field, and its influence on the atom with which it interacts.

In this paper we have exhibited new features of the coherent-state Jaynes-Cummings model. Principal among these new features is the occurrence of revivals, i.e., partial recorrelations of the collapsed initial state. We have shown that these revivals occur periodically to a first approximation, with period T_R equal to $2\pi\bar{n}^{1/2}t_0$, where t_0 is the Gaussian local collapse time. We have found an expression for t_0 that is valid on or off resonance. Collapse occurs, even though the interacting model Hamiltonian is Hermitian, because the initially coherent-field state is a superposition of eigenstates of the free Hamiltonian with quasirandom amplitudes and phases.

It is the incompletely random character of this superposition that permits revivals to occur. In our study of the dipole moment we showed that two widely different revival periods can be observed. The second period is longer than the first by the factor $4\bar{n}$. We expect that even longer recorrelation periods can be identified.

The question arises whether or not the coherent-state Jaynes-Cummings model is suitable for a discussion of irreversibility. Even if $\bar{n}$ is only as large as 10, it is clear from Sec. III that the short-time behavior is far from monotonic, and thus not described by the simplest Pauli-type master equation. However, the short-term coherent Rabi oscillations do decay in the time t_0, and do not recur until the much longer time $T_R = 2\pi\bar{n}^{1/2}/\lambda$.

Van Hove[17] has pointed out that an irreversible Pauli-type master equation can be taken as valid for a wide class of systems assuming only initially (and not repeatedly) randomized phases. While the coherent-state Jaynes-Cummings model does not have all of the features required by Van Hove, being characterized by discrete rather than continuous quantum numbers, and by not-quite-random initial phases and amplitudes, we may still ask how close does the model's behavior come to being approximately irreversible in the Van Hove limit: $\lambda \to 0$, $t \to \infty$, $\lambda^2 t = \text{const}$.

Actually, at least two types of quasi-irreversible behavior appear to be contained in the Jaynes-Cummings model. The first is evident in the collapse between $t = 0$ and $t = t_0$. If the first revival is pushed into the indefinite future, so that $t \ll T_R \to \infty$, while

$$\lambda \to 0 \quad \text{and} \quad \lambda^2 T_R = \text{const}, \tag{5.1}$$

it follows that the constant in (5.1) can be interpreted physically. From (5.1) and (3.16) we find

$$(4\lambda^2\bar{n} + \Delta^2)^{1/2} = \text{const}, \tag{5.2}$$

which is equivalent to a constant Rabi frequency for the interaction. That is, one can say that the first type of quasi-irreversibility is automatically encountered in the "thermodynamic" limit ($V \to \infty$, so that $\lambda \to 0$) if the Rabi frequency is fixed. It is, however, also automatically true as $\lambda \to 0$ that the "irreversible" decay, characterized by the time $t_0 \sim \lambda^{-1}$, requires a longer time to be accomplished. In the limit $\lambda \to 0$, collapse does not occur at all and the temporal behavior of both inversion and dipole moment consists entirely of perfectly periodic Rabi oscillations.

The existence of a second type of quasi-irreversible behavior is suggested by the observation that the revivals shown, for example, in Fig. 3(b) get broader and broader. Eventually neighboring recorrelations overlap. The overlap occurs sooner if $\bar{n}$ is smaller. An example of this kind of overlap is shown in Fig. 10. We do not have an accurate expression for the width of a recorrelation envelope, and so cannot compute for a general value of $\bar{n}$ the time when sufficient overlap occurs to produce enough scrambling of the neighboring recorrelations to permit one to say that "real" irreversibility has set in. The times appropriate to this second type of irreversibility might correspond to the times when a Pauli-type master equation is valid in some average sense.

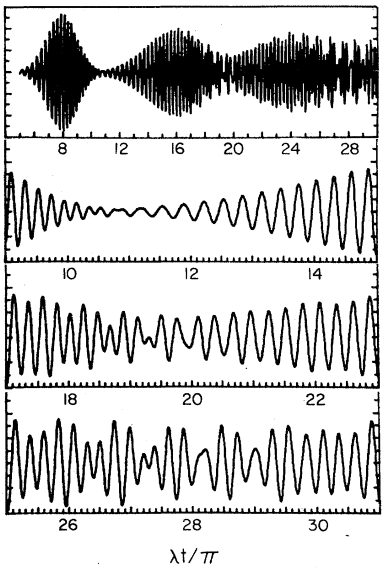

FIG. 10. Overall and close-up views of the earliest three revivals of $w(t)$ for $\bar{n}=16$, $m=-1$, and $\Delta=0$. The sequence, from top to bottom, shows an overall view of the first three revivals $4 \leq \lambda t/\pi \leq 30$, and closeups of the intermediate regions between the maxima of each two consecutive revivals for $9 \leq \lambda t/\pi \leq 15$, $17 \leq \lambda t/\pi \leq 23$, and $25 \leq \lambda t/\pi \leq 31$. In addition to features explained in Fig. 3, the growing spread and the resultant overlapping of the revivals of $w(t)$ as it evolves in time are clearly shown in the first picture. The changing character of the overlap region is shown in the three lower pictures. The uniformly oscillating almost nonoverlapping first and second revivals are shown in the second picture. In the third picture, partial overlapping of the second and third revivals is accompanied by some irregularity of the oscillations in the overlapping region, and in the fourth picture one sees the almost complete overlapping of the third and fourth revivals where quasirandom oscillations are now the dominant feature.

Despite the more or less complete zero-order description of collapse and revival that we have given for the coherent-state Jaynes-Cummings model, it is apparent that much more needs to be done. We have begun a study[18] of two-time expectation values in the model, and of the atomic emission spectrum. It will also be necessary to examine the question of Poincaré recurrences carefully: How closely can one bound the time $T(\epsilon)$ at which dynamical variables return to within ϵ of an earlier value? Is there an infinite hierarchy of revival times? Under what circumstances, if any, does the model's behavior coincide with the behavior predicted by a master equation?

Finally we point out a comparison of the results obtained from the Jaynes-Cummings model in what are naturally denoted "classical" and "quantum" initial states. The classical state corresponds to initial preparation of the field in a coherent state with amplitude α, whereas the corresponding quantum state arises from initial preparation in an n-photon state, with $n=|\alpha|^2$. The dynamic behavior of the atomic inversion subsequent to these different preparations is almost exactly opposite the behavior that their names suggest. That is, the classical coherent state, with well-defined electric-field phase, produces collapsing Rabi oscillations, as we have shown in Sec. III. The quantum n-photon state, with completely undefined electric-field phase, on the other hand, is well known[1,3,15] to produce periodic and nondecaying Rabi oscillations. The latter, not the former, is exactly the response of the atom to excitation by an external and completely classical electric field.[15]

This comparison of responses to classical and quantum preparations of the initial quantum state, in contrast with the response to the corresponding fully classical electric field, is significant. It shows, of course, that the quantum-classical correspondence is not straightforward. But it also shows what major differences can occur in the kind of coherence effects to be found in interacting and free systems. The coherence properties of both classical and quantum-mechanical free-fields are well studied, and well known to have strong similarities. The coherent-state Jaynes-Cummings model appears ideal for studies of the long-time coherence properties of interacting fields. We will return to this subject in later papers.

ACKNOWLEDGMENTS

We thank P. Meystre and S. Stenholm for interesting conversations and information about earlier work with the coherent-state Jaynes-Cummings model, and H. I. Yoo for consultation concerning the final forms of (3.19) and (3.20). This work was partially supported by the U. S. Department of Energy. One of us (J.J.S.) would like to thank the Mary Street Jenkins Foundation for financial support, and one of us (N.B.N.) acknowledges the support of the International Research and Exchanges Board.

*IREX Visiting Scholar, 1978–1979, permanent address: Moscow Engineering Physics Institute, Moscow 115409, USSR.

†Mary Street Jenkins Foundation Fellow, Puebla, Mexico.

[1]E. T. Jaynes, Microwave Laboratory Report No. 502, Stanford University, 1958 (unpublished).

[2]By rotating wave approximation one can understand the neglect of terms in the interaction Hamiltonian that are not approximately energy-conserving in lowest order. A more pictorial view based on spin precession is given in may texts on resonance physics, for example, Ref. 15, Chap. 2.

[3]E. T. Jaynes and F. W. Cummings, Proc. IEEE 51, 89 (1963).

[4]A preliminary account is given in J. H. Eberly, N. B. Narozhny, and J. J. Sanchez-Mondragon, Phys. Rev. Lett. 44, 1323 (1980).

[5]M. Tavis and F. W. Cummings, Phys. Rev. 188, 692 (1969).

[6]The papers of R. Weiss, Helv. Phys. Acta 46, 546 (1973), and G. Compagno and F. Persico, Phys. Rev. A 15, 2032 (1977), give extensive references to other work with the N-atom one-mode problem, notably by Mallory, Scharf, Walls and Barakat, and Bonifacio and Preparata.

[7]A. Quattropani, Phys. Kondens. Mat. 5, 318 (1966).

[8]F. W. Cummings, Phys. Rev. 140, A1051 (1965).

[9]S. Stenholm, Phys. Rep. 6, 1 (1973), p. 66.

[10]T. von Foerster, J. Phys. A 8, 95 (1975).

[11]A. Faist, E. Geneux, P. Meystre, and A. Quattropani, Helv. Phys. Acta 45, 956 (1972); P. Meystre, E. Geneux, A. Faist, and A. Quattropani, Lett. Nuovo Cimento 6, 287 (1973); E. Geneux, P. Meystre, A. Faist, and A. Quattropani, Helv. Phys. Acta 46, 457 (1973).

[12]P. Meystre, A. Quattropani, and H. P. Baltes, Phys. Lett. 49A, 85 (1974).

[13]P. Meystre, E. Geneux, A. Guattropani, and A. Faist, Nuovo Cimento 25B, 521 (1975).

[14]J. R. Ackerhalt, Ph.D. thesis, University of Rochester, 1974 (unpublished). See also J. R. Ackerhalt and K. Rzażewski, Phys. Rev. A 12, 2549 (1975), Sec. IV D.

[15]L. Allen and J. H. Eberly, *Optical Resonance and Two-Level Atoms* (Wiley, New York, 1975), Chap. 7.

[16]See, for example, *Handbook of Mathematical Functions*, edited by M. Abromowitz and I. A. Stegun, U.S. Dept. of Commerce (U.S. Govt. Printing Office, Washington, 1964), p. 806.

[17]L. Van Hove, Physica (Utrecht) 21, 517 (1955).

[18]J. Sanchez-Mondragon, N. B. Narozhny, and J. H. Eberly, J. Opt. Soc. Am. 69, 1414 (1979).